Geosystems and Geoenvironment 1 (2022) 100007

Contents lists available at ScienceDirect

Geosystems and Geoenvironment

journal homepage: www.elsevier.com/locate/geogeo

Episodic habitation and abandonment of Neolithic civilization sites in the Vaigai River Basin, Southern India

Mu. Ramkumar[a,*], K. Balasubramani[b], K. Kumaraswamy[c], M. Santosh[d,e], Priyadarsi D. Roy[f], A. Manobalaji[a], K.J. Juni[a], R. Nagarajan[g,h], Rajveer Sharma[i], Pankaj Kumar[i], Sundeep Chopra[i], N.A. Siddiqui[j], C. Ramachandran[a], S. Leo George[b]

[a] *Department of Geology, Periyar University, Salem, India*
[b] *Department of Geography, Central University of Tamil Nadu, Thiruvarur, India*
[c] *Department of Geography, Bharathidasan University, Tiruchirappalli, India*
[d] *School of Earth Sciences and Resources, China University of Geosciences, Beijing 100083, China*
[e] *Department of Earth Sciences, University of Adelaide, Adelaide, SA 5005, Australia*
[f] *Instituto de Geología, Universidad Nacional Autónoma de México, Ciudad Universitaria, Ciudad de México, CP, 04510, Mexico*
[g] *Department of Applied Geology, Curtin University Malaysia, Miri, Sarawak, 98009 Malaysia*
[h] *Curtin Malaysia Research Institute, Curtin University Malaysia, Miri, Sarawak, 98009 Malaysia*
[i] *Inter University Accelerator Centre, New Delhi, India*
[j] *Department of Geosciences, Universiti Teknologi PETRONAS, Seri Iskandar 32610, Malaysia*

A R T I C L E I N F O

Article history:
Received 24 September 2021
Revised 6 October 2021
Accepted 11 October 2021

Keywords:
Ancient settlements
Climate change
Extreme climatic events
Forced abandonments
Habitation continuum
Vaigai civilization

A B S T R A C T

Recent studies have unearthed and recovered multiple sites with evidences of past human habitations in terms of ceramic, metal, precious stone, jewel, and stone tool industries and places of varied methods of burial and worship are being unearthed at different stratigraphic levels from floodplains of the Vaigai River Basin, Southern India. In this contribution, we present high-resolution ^{14}C chronology of the archaeological artefacts, cultural evidence and the textural characteristics of sediments collected from the excavated pits. These data along with the information on regional geology, geomorphology, sedimentary facies, texture, petrography, and mineralogy constrain the older phase of the Vaigai River Basin Civilization to be microlithic in age, followed by affirmative evidence of ca. 5511-5147 BCE (7455-7091 cal yr BP). This was followed by few more colonization/cultural/habitation sites/surfaces at ca. 2976-2961 BCE (4938-4908 cal yr BP), 1860-1489 BCE (3543-3503 cal yr BP),530-390 BCE (2435-2314 cal yr BP), 596-629 CE (1353-1321 cal yr BP) and post 1225-1312 CE (729-619 cal yr BP). These are designated as habitation sites/surfaces namely HS-1, HS-2, HS-3, HS-4, HS-5 and HS-6, respectively. Evidences of urbanism, industrial and leisure activities besides cohabitation of at least three groups that practiced mutually exclusive burial customs are documented. Microlithic tools and buried habitation stages, together with the prevalence of modern habitations, make this basin unique with human occupation at least since the mid-Holocene. Major shifts of the trunk channel of the Vaigai River, perhaps associated with flood events, marooned/buried/destroyed the ancient habitation sites that forced the inhabitants to abandon old sites and led to the reestablishment of newer ones. Inevitable dependence of the ancient societies on the riverbanks and the flood plains for settlements and livelihood compounded with the lack of knowledge on extreme climatic events possibly caused the decimation of several settlements of this important civilization from south India.

1. Introduction

Natural climate change as well as extreme weather events such as floods and droughts exert control over erosion-transportation-deposition processes and impact landscape development (Bookhagen et al., 2005). Settlements of ancient civilizations along water bodies such as rivers, lakes and along coasts were under the vagaries of seasonal-short and/or long-term climatic changes and natural hazards (Singh et al., 2017). Catastrophic flooding, associated with extreme weather conditions also result in calamity, forcing either abandoning of these habitation sites for

* Corresponding author.
E-mail address: muramkumar@yahoo.co.in (Mu. Ramkumar).

https://doi.org/10.1016/j.geogeo.2021.10.002

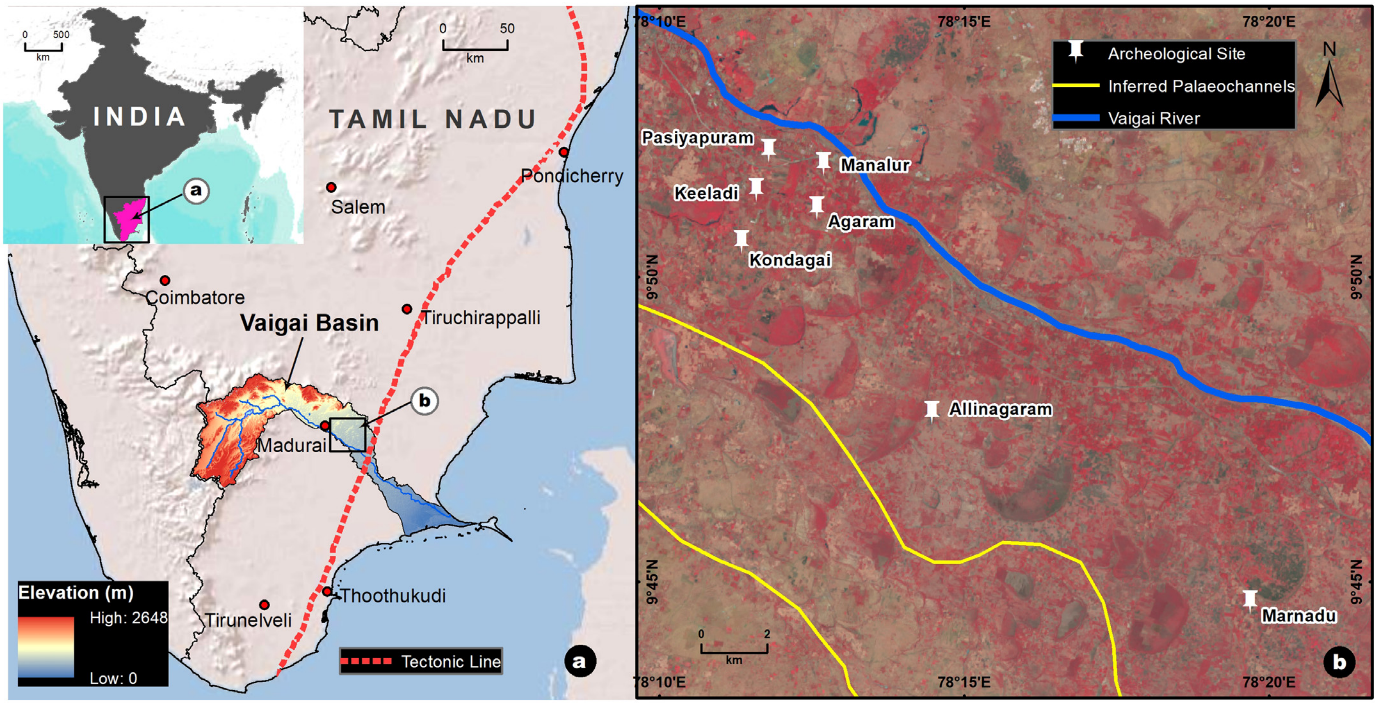

Fig. 1. Location of the Vaigai River Basin and the archaeological sites examined/excavated. a: Location of the study area within the Vaigai River Basin, embedded on a Digital Elevation Model. It also depicts the inherited nature of the river basin. b: Location of archaeological sites wherein natural exposures were examined and excavations were made. Yellow lines show the paleochannels inferred through image processing and interpretation. (For interpretation of the references to color in this figure legend, the reader is referred to the web version of this article.)

survival and/or perishing in calamity (e.g., Ramkumar et al., 2018, 2019). The relationship between climate change and major cultural transitions was extensively evaluated on the Mayan civilization with about 3-13 million habitants that flourished during <200 CE in the Yucatan Peninsula of southeast Mexico (P.D. Roy et al., 2017). Multi-year droughts with intervals of 40-50 years between 750-950 CE have been linked to the abandonment of densely populated urban centers (Haug et al., 2003; Medina-Elizalde et al., 2010; Roy et al., 2017). Deposition of authigenic calcite between ca. 944-1096 CE through droughts, and aeolian activity also reflect dry conditions, coeval with the abandonment at another Mesoamerican urban center at Xochicalco with an estimated maximum population of about 9-15 thousand (Roy et al., 2020). A recently published paleoclimate time series dataset from a speleothem oxygen isotope composition from Northern India covering the past 5700 years shows a possible connection between climate change and the decline of the Indus Valley Civilization at ca. 1900 BCE (Malik, 2020). Erratic rainfall lasting for about 900 years during this interval in the north-west Himalayas dried up water supply to the Indus Valley located at the north-west India and south-east Pakistan. Nevertheless, human responses to these climatic fluctuations varied considerably from region to region. In Gujarat, the faunal analyses and isotopic data in tooth enamel did not show any evidence for significant changes in pastoral landuse practices through this drought interval, indicating considerable resilience on the part of local pastoral producers (Chase et al., 2020).

The sophisticated monitoring and forecasting equipment and infrastructure of the modern era can mitigate the effects of extreme climatic events to some extent. These facilities were not available to our ancestors who faced similar natural hazards and were prone to loss of life and infrastructure, including settlements (e.g., Nigam et al., 2016; Nigam and Chaturvedi, 2006; Roy and Sethumadhav, 2014; Rao, 1991; Roy et al., 2017; Similox-Tohon et al., 2006; Singh et al., 2017; Valdiya, 2008). Folklore, rock art, culvert and the documented evidence including archaeological artefacts unequivocally stand testimony to the vulnerability and periodic susceptibility to natural catastrophes, especially coastal and fluvial flooding (Rao, 1991; Roy et al., 2017; Ramkumar et al., 2018, 2019). Influences of climatic shifts on streamflow have the potential to increase/decrease sediment flux and thus, affect riverbed elevation by altering flood frequency and magnitude (Ramkumar, 2009; Slater and Singer, 2013). These unforeseen responses of bed elevation to exogenic forcing and climate change have important implications for survival-demise/burial of the ancient civilization sites located along riverbanks (Slater and Singer, 2013; Thakur et al., 2016; Ramkumar et al., 2015a, 2015b, 2018, 2019; Sofia and Nikolopoulos, 2020). In this paper, we document the episodic channel avulsion, perhaps associated with extreme climatic events and resultant episodic abandonment and resettlement in the Vaigai River Basin, Southern India.

2. Location and regional setting

The southern Indian Shield is a mosaic of several crustal blocks with a variety of geological signatures engrained during different intervals ranging since the early Archaean (GSI, 1975; Santosh et al., 2020; Gao et al., 2021). The Vaigai River, located in the Tamil Nadu state of southern India flows on an antecedent narrow valley (Fig. 1a), and its directional change imparted by prevalent tectono-morphological events under the influence of inherited Proterozoic structures is unique to the region (Ramkumar et al., 2016, 2019). However, the location of deltahead at/or near to the tectonic line suggested a shared/common mechanism for this fluvial basin with that of adjacent basins. Incision of paleo-alluvial fills, development of Miocene-Pliocene kankar/paleosol, recycling of paleosol and development of Holocene-to-Recent soil, and historical changes of river courses occurred in response to tectonic events and short-long term climatic reversals (Ramkumar et al., 2016, 2019). The Vaigai River Basin consists of 10 sub-basins, covers an area of about 7000 Ha and lies within the tropical monsoon

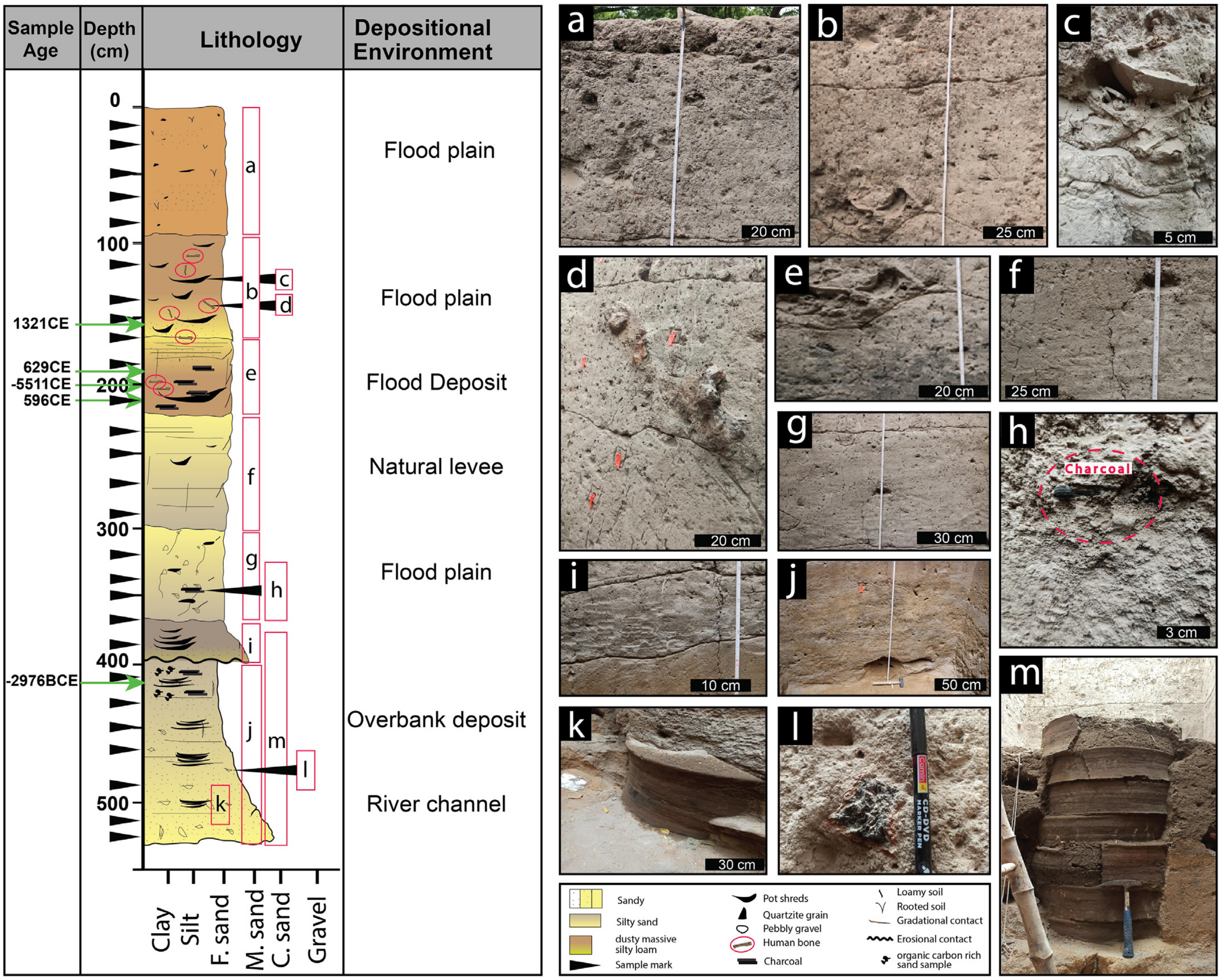

Fig. 2. Litholog and photolog of the Agaram Pit. Stratigraphic locations of the sediment, artefact and bone samples are also marked in the log and shown in the associated photographs. The stratigraphic locations of the photographs in the litholog are marked by labeled bars.

climatic zone with an average annual rainfall of about 775 mm (http://nwm.gov.in/sites/default/files/Vaigai_Basin-17.07.17.pdf). The Southwest (SW) monsoon, spanning from June-September and the Northeast (NE) monsoon, spanning from October-December bring rainfall to this basin. Most of the rainfall of this basin occurs in a short spell (about 40 days in a year) during the NE monsoon season.

3. Methods and materials

3.1. Excavation and sampling

The presence of man-made structures and artefacts in the subsurface was affirmed through conventional, geophysical and visual interpretation and image processing of remotely sensed data. Based on these studies, we determined locations for the examination of natural and anthropogenic structures, lithofacies characteristics and sediment/soil/artefact sampling. The methods employed for site determination, field logging and sampling protocols are detailed in Ramkumar et al. (2021). Two pits of archaeological excavation, one at Agaram (Fig. 2) and another at Keezhadi (Fig. 3) were chosen for sediment and artefact sampling. After photographing and logging, the sediment samples were collected at 20 cm intervals, in addition to artefacts and archaeological remains (Fig. 6). Approximately 1 kg of sample from each stratigraphic location was packed in airtight PVC bags, labeled and transported to the laboratory. A total of 28 sediment samples for granulometric analysis and a charred bone clast for petrographical, mineralogical and ^{14}C analyses were collected from the Agaram Pit. Few pot shreds, paleohearth, and chunks of charcoal were also recognized in this pit (among which one turned out to be a charred bone during laboratory examination and subsequent petrographic analyses, details of which are presented in the petrography section) and sampled (see Fig. 2 for the stratigraphic locations and field photographs) for ^{14}C analyses. Five organic carbon rich-layers were recognized in the Keezhadi pit (Fig. 3) and were sampled for granulometric and ^{14}C analyses.

3.2. Granulometric analysis

Granulometric analysis of the sediments in the Sedimentology lab of the Department of Geology, Periyar University, and computation of textural parameters were attempted following the procedures detailed in Ramkumar et al. (2000) and Ramkumar (2001,

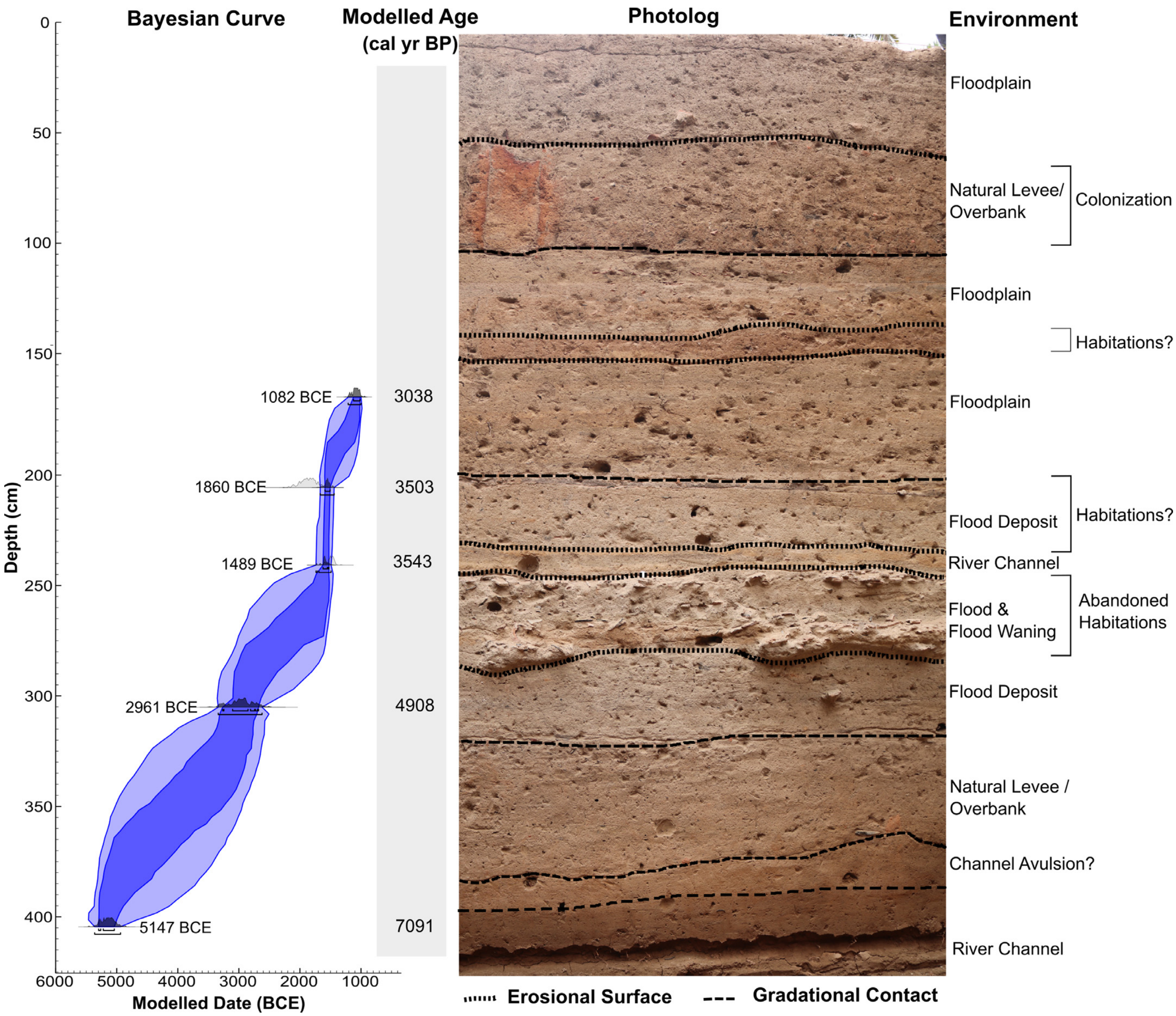

Fig. 3. Fieldphotolog of the Keezhadi pit. Environmental interpretations, stratigraphic locations of samples and ^{14}C calibrated age with Bayesian curve are annotated. Facies and other characteristics indicate the episodic habitation followed by abandonment principally under the influences of catastrophic floods. Changing environmental conditions, as reflected by the stratigraphic successions of geomorphic units also indicate stream avulsion events on a temporal scale. In the Bayesian curve, dark blue shade indicates 95.4% probability and the light blue shade indicates 68.3% probability. (For interpretation of the references to color in this figure legend, the reader is referred to the web version of this article.)

2007, 2015b) and are briefly presented herein. The samples were air-dried, thoroughly mixed, homogenized and cone and quartered to obtain approximately 50 gm of sediment subsample. Large pieces of shell fragments, organic material or pebbles were removed. These subsamples were transferred to a pre-cleaned glass beaker. The samples were cleaned through three stages of treatments by hydrogen per oxide, 10% v/v HCL and quasi-distilled water to remove organic matter, shell calcite and other contaminants. These subsamples were then dried in an air-oven overnight at 60 °C and weighed and dry-sieved in an automated sieve-shaker with ASTM test sieve sets of ½ Ø intervals for about 20 min. The separated size classes of sediments were then weighed and tabulated. These data were converted into ¼ Ø intervals with a computer algorithm (Ramkumar, 2001, 2007; Ramkumar et al., 2000, 2015b), and then cumulative percent according to Ø interval were calculated and plotted in a semi-log graph sheet for generating requisite data to compute the graphic mean (Mz), the standard deviation (SD), the skewness (S_K) and the kurtosis (K_G). In addition, the input data required for a few bivariate and other discriminant plots of environmental (Friedman, 1967; Moiola and Weiser, 1968), energy (Stewart, 1958) and transport mode (Passega, 1957) interpretations were also generated from the plots of cumulative percent of the sediment samples.

3.3. *Petrography*

Polished sections and petrographic thin sections were prepared in the sedimentology lab of the Department of Geology, Periyar University, from the charred bone clast recovered from the Agaram pit. Chips were cut from the bone clast at right angles in order to examine the bone structure at longitudinal and cross-sections. The cut-chips measuring 30 mm X 20 mm were polished and examined under reflected light binocular microscope at various magnifications and then photographed. These chips were then mounted in glass slides, polished further into thin sections (∼30 µm) for examination under the polarized light in the petrographic microscope for documentation of microstructure, texture, mineralogy and other parameters.

3.4. Mineralogy

A total of 8 samples from both the pits were powdered using an agate mortar and pestle to <63 µm size and the powders were analyzed for mineralogy through X-Ray Diffraction. Analyses were performed in the IUAC (Inter-University Accelerator Centre), New Delhi. The samples were measured at 2 theta (θ) angles between 3° and 80° continuously with a step size of 0.01°. The resultant diffractograms were examined with the help of HighScore Software manufactured and licensed by Panalytical B.V., for peaks, patterns and phases to identify mineral species present in the samples.

3.5. Chronology through ^{14}C analyses

A total of 15 samples (charcoal, charred bone clast, bone, and organic carbon-rich sediment) were measured for total organic carbon, and 14 of them were considered for radiocarbon dating on the basis of available organic carbon contents. Out of these, only 10 samples were qualified for the analysis after the physical examination. They were chemically pretreated using the ABA (Acid-Base-Acid) protocol. Sediment and charcoal samples were mixed with 15 mL 0.5 M HCl and kept for 3 h on a thermo-shaker at 60 °C and 700 rpm to remove carbonates. After acid treatment, samples were cleaned with deionized (DI) water up to pH 7. To remove humic acid, samples were treated with 15 mL 0.1 N NaOH at 60 °C and 700 rpm for 2.5 h. Again, after cleaning with DI water, the samples were pretreated with 0.5 M HCl at 60 °C and 700 rpm for 1.5 h to remove any absorbed CO_2 during base treatment. After cleaning with DI water, the samples were freeze-dried for 8-10 h and subsequently graphitized using an Automated Graphitization Equipment (AGE) at IUAC.

Bone sample (n = 1) was first cleaned using ultrasonic, dried and then powdered to < 63 µm size. The powdered sample was demineralized using 0.2 M HCl and stored for 10 days in a refrigerator. Samples were monitored for effervescence continuously and acid was replaced with fresh acid after 24 h. After demineralization, the samples were cleaned with DI water and mixed with 10 mL 0.1N NaOH and kept for 30 minutes at room temperature to remove any humic acid contamination. After rinsing with DI water up to pH 7, 0.2 M HCl was mixed into the sample and the mixture was kept for 30 minutes at room temperature to allow reaction for removal of CO_2 possibly absorbed during the base treatment. The sample was finally washed with DI water and again mixed with DI water and 3-4 drops of 0.5 M HCl to make solution pH 3 and kept for gelatinization at 90 °C for 24 h (Longin, 1971). The gelatinized (collagen) sample was freeze-dried and graphitized using AGE.

The ^{14}C measurements were made using AMS (Accelerator Mass Spectrometry) at IUAC, following the procedures described in Sharma et al., 2019. $^{14}C/^{12}C$ ratio in the graphite produced after graphitization was measured in all the samples using XCAMS (The compact Carbon Accelerator Mass Spectrometer extended for ^{10}Be and ^{26}Al) and sample ratios ($^{14}C/^{12}C$) were converted to radiocarbon ages as described in Stuvior and Polach (1977). All the radiocarbon ages (BP) were calibrated using OxCal (v 4.4.4) software using IntCal 20 calibration curve and converted into calendar year before present (cal yr BP) scale. Bayesian age depth modeling was also done using OxCal (v 4.4.4) software (Bronk Ramsey, 2009)

4. Results

4.1. Facies and textural characteristics

Litholog of the Agaram pit shows the occurrence of massive, poorly sorted, fining upward, fine sand deposit of riverine origin (Fig. 2) at the bottom part of the excavated surface. This facies grades to the overbank deposit of massive, poorly sorted, fine sand with appreciable quantities of carbon, possibly derived from ash and charcoal. This bed has a non-depositional and erosional surface at the top, and it is overlain by loamy soil facies of flood plain. The floodplain facies are represented by massive, poorly sorted, fine sand with intermittent non-depositional surfaces. A prominent non-depositional surface separates this facies from the overlying massive, thick, silty sand of natural levee. This facies have an erosional surface at the top and is overlain by flood deposits of poorly sorted, fine sand in which scattered bone clasts occur. It shows gradational contact with flood plain deposits of poorly sorted, fine sand. This sequence contains evidence for human habitation, such as ring-well and hearth, etc. The lithology at Keezhadi pit has similar facies representing river channel-overbank-floodplain-natural levee-floodplain (Fig. 3). The frequency of the carbon-rich layers, however, is more, perhaps associated with flooding and human habitation.

Texturally, the sediment samples collected from both the pits are mainly fine sand, interspersed with very fine sand towards the lower part and interlayers of medium sand and coarse sand at the top. Stratigraphic representations of the textural parameters such as mean size (Mz), standard deviation (SD), skewness (S_K) and kurtosis (K_G) appear to be monotonous at the bottom that changes to high-frequency variations in the middle and extreme variability at the top (Fig. 4). Except for three with moderate sorting, all the samples are poorly sorted. The skewness of the studied samples shows a range from fine skewed to very coarse skewed. Most of the samples are leptokurtic to extremely leptokurtic. Sediments representing the erosional surfaces and intense human-habitation surfaces are coarse and very coarse-skewed. A gradual fining upward nature superimposed on episodic changes in these textural characteristics indicates an overall long term linear trend of fining (Fig. 4a), shift from moderate to poor sorting (Fig. 4b), change from very coarse skewed to symmetric-fine skewed (Fig. 4c) and change from mesokurtic to very leptokurtic (Fig. 4d). The polynomial trend shows a significant shift in sediment characteristics (Fig. 4).

All the samples fall within riverine fields of the discriminant diagrams (Figs. 5a and 5b) of Friedman (1967) and Moiola and Weiser (1968). In Stewart (1958) plot, all the samples are within river process and are scattered near deposition under quite water fields (Fig. 5c). Based on relative maturity of the sediments following Glaister and Nelson (1974) plot, the samples are within immature range and are distributed within braided bar, point bar and delta front microenvironments/geomorphic units (Fig. 5d). In the discrimination diagram of Passega (1957), the samples suggest prevalent dominant transportation by suspension with rolling mode (Fig. 5e).

4.2. Microstructure and pore-fills

Partially rounded external morphology of the charred bone clast is discernible from megascopic observation. Examination of the polished and thin sections of this charred bone clast under reflected and polarized light (Fig. 6) revealed that the microstructures are completely obliterated by burning and the pores within the original microstructures are filled by fine-silt to sand-sized clastic grains of quartz, plagioclase feldspar, oxidized/oxide-coated ferromagnesian mineral grains, and calcitic cement and neomorphic spars of multiple generations (Ramkumar, 2008;

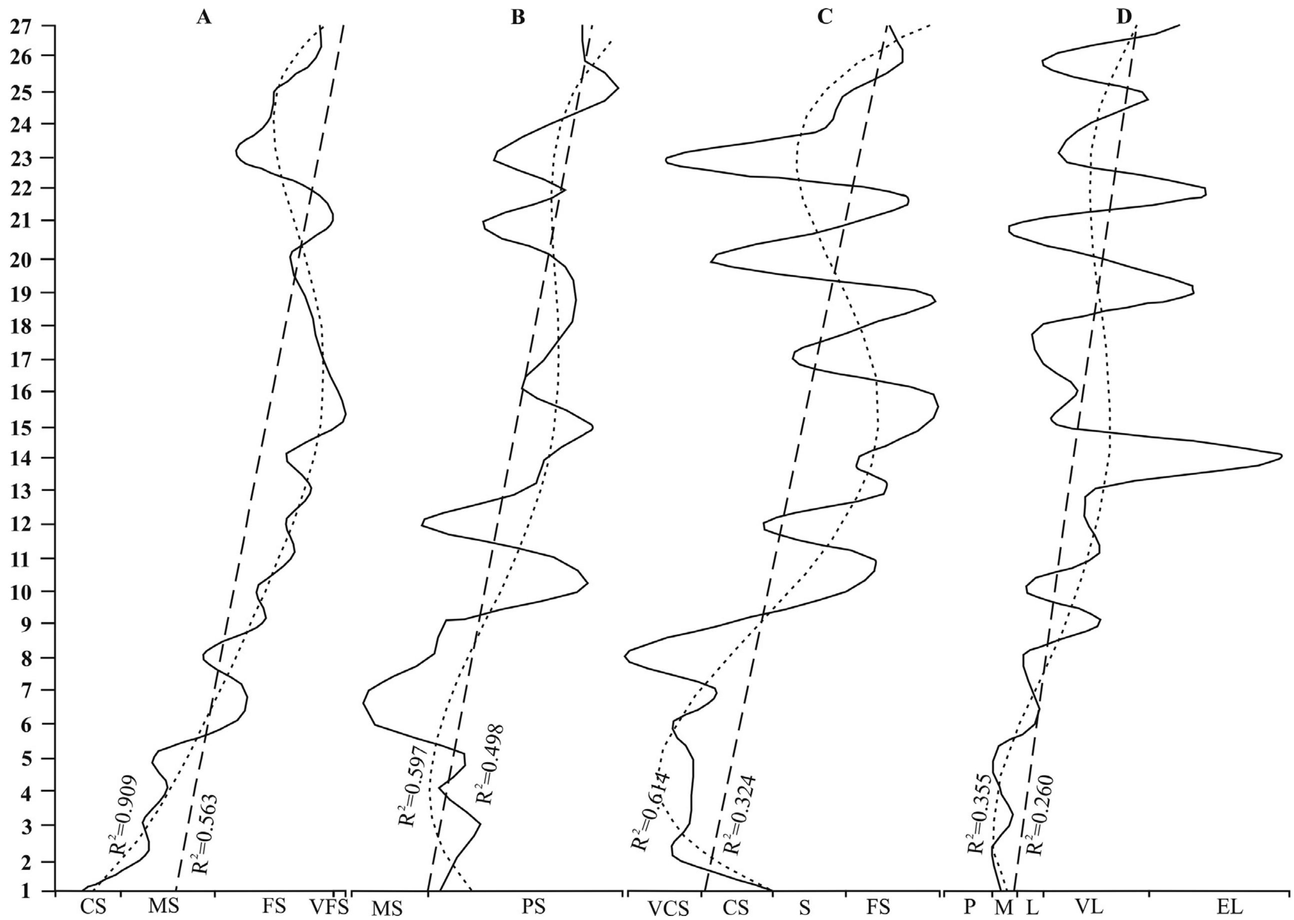

Fig. 4. Stratigraphic variations of the textural parameters, Agaram section. a: Mean size; b: Standard Deviation; c: Skewness; d: Kurtosis. The solid line shows the absolute values the dashed line shows the linear trend and the dotted line shows the polynomial trend.

Ramkumar et al., 2013), and irregular-shaped patches of iron-oxide fillings. The micropores are filled with cement spars of rhombic calcites that depict compromise structures (sensu, Bathurst, 1972, 1987) and gradual increase in spar size toward the centre, a trait affirmative of cementation under meteoric conditions (e.g., Bathurst, 1972, 1987; Ramkumar, 2008) of diagenesis. Cross-cutting fractures of the microstructure pore-fills are filled with later stage calcite cement spars with various stages of weathering and destructive neomorphism (e.g., Bathurst, 1972, 1987). Reduction of pore-fillings and concomitant increase of empty pores of the original bone microstructure are recognized from the outer periphery towards the centre. Similarly, the iron-oxide coating along the walls is ubiquitous along the periphery of bone clast that shows distinct reduction toward the centre to become completely absent at the centre.

4.3. Mineralogy

The mineral species identified are presented in the Table 1 which shows ubiquitous occurrence of quartz as the dominant mineral, followed by feldspars (plagioclase feldspars: Albite and oligoclase and K-Feldspar–orthoclase and microcline), can be recognized. Feldspars are followed by the occurrences of the ferro-magnesian minerals such as orthopyroxene and clinopyroxenes. Muscovite mica and its weathering products such as illite and montmorillonite clays are recognized. Minor to noticeable amounts of calcite, and apatite followed by insignificant amounts of lanthanite, zirkelite and sapphirine also occur. Mineralogical data along with petrographic observations suggested the presence of hematite as iron oxide coatings on the grains and pore walls.

4.4. Chronology

Agaram pit: Except for one bone clast, all the radiocarbon ages are stratigraphically consistent (Table 2). The bone at 170 cm depths from this pit yielded the youngest (1312 CE; 619 ± 39 cal yr BP) radiocarbon age of this sequence (Table 2). However, the charcoals of the same sequence at depths of 216 cm and 198 cm yielded comparable ages of 596 CE (1353 ± 25 cal yr BP) and 629 CE (1321 ± 17 cal yr BP). Both were collected from a layer of flood deposit (Fig. 2). The bulk organic carbon constrains the sediment at 430 cm depth to 2976 BCE (4938 ± 84 cal yr BP). Charred boneclast is recovered from sediments at 200 cm depths representing the oldest (5511 BCE; 7455 ± 73 cal yr BP) of this sequence and it was recovered from the same layer of flood deposit indicating its reworked nature.

Keezhadi pit: The deepest sediment layer at 325 cm was deposited at ca. 5147 BCE (7091 ± 109 cal yr BP) (Table 2). Other sediments of this pit show a systematic younger depositional age with decreasing depths between 2961 BCE (4908 ± 192 cal yr BP) and 1082 BCE (3038 ± 57 cal yr BP) (Fig. 3). The lower and upper limits of the bulk organic sediments at 240 cm and 205 cm depths are almost similar and the stratigraphically inconsistency of both these sediment layers might represent the reworking of older sediments in the flood deposit at 205 cm depth.

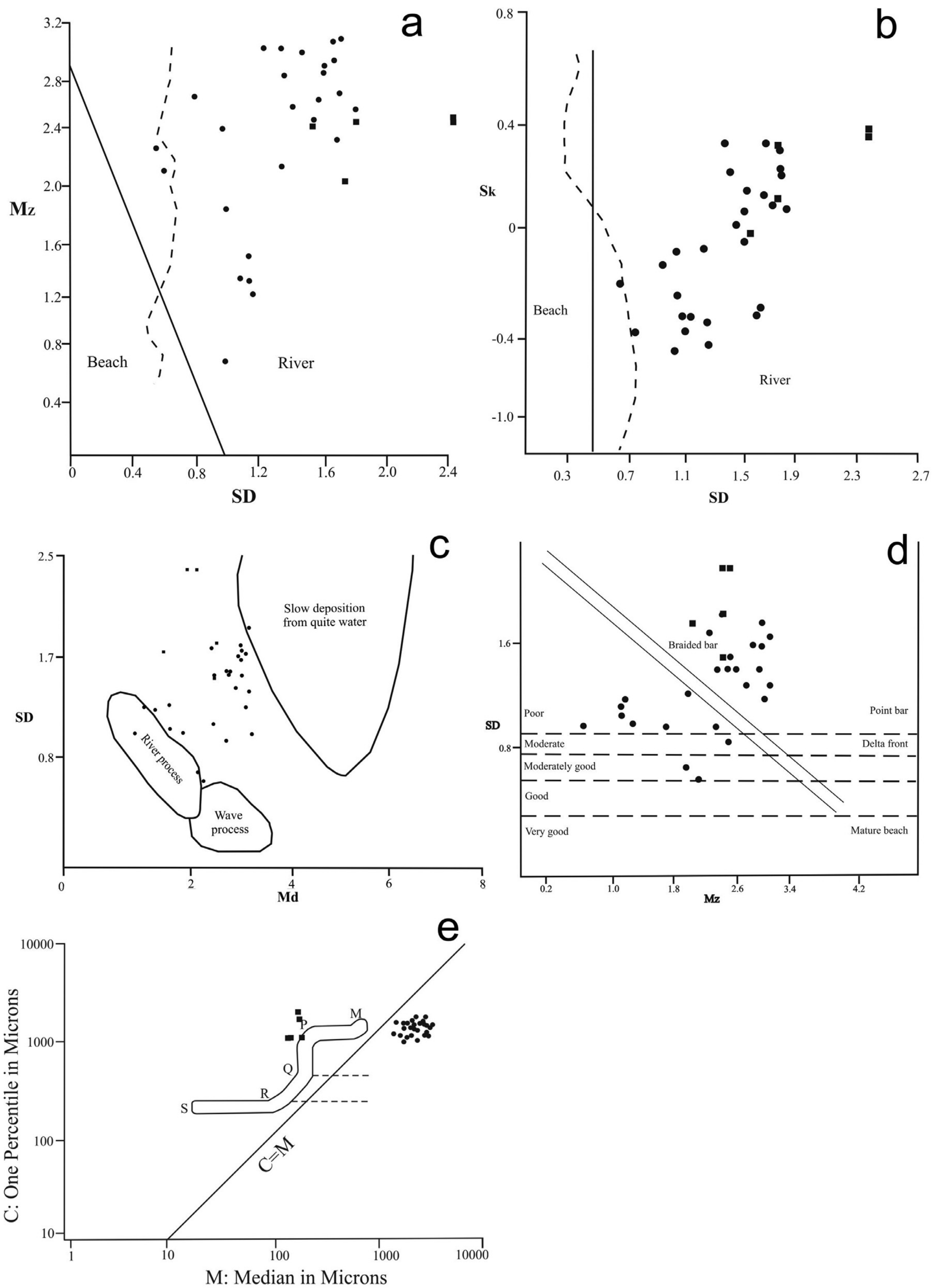

Fig. 5. Discriminant diagrams of sediment origin, energy and environmental setting. The samples from the Agaram pit are shown in solid circles and the samples from the Keezhadi pit are shown in solid squares. A distinction of plotting areas/locations/regions of the samples from two different pits suggests differences in transport mode, depositional energy, and depositional environmental settings. a: Environmental discrimination based on mean size and standard deviation (after Friedman, 1967 and after Moiola and Weiser, 1968); b: Environmental discrimination based on skewness and kurtosis (after Friedman, 1967 and after Moiola and Weiser, 1968); c: Determination of intensity of energy conditions and directional movement of sediments (after Stewart, 1958); d: Determination of relative maturity and depositional setting (after Glaister and Nelson, 1974); e: Determination of modes of sediment transport (after Passega, 1957). The field M-O indicates sediments that are transported by rolling, O-P rolling and suspension, P-Q suspension with rolling, Q-R graded suspension, and R-S indicates uniform suspension. The upper dashed horizontal line indicates maximum grain size transported by graded suspension and the lower dashed horizontal line indicates maximum grain size transported by uniform suspension.

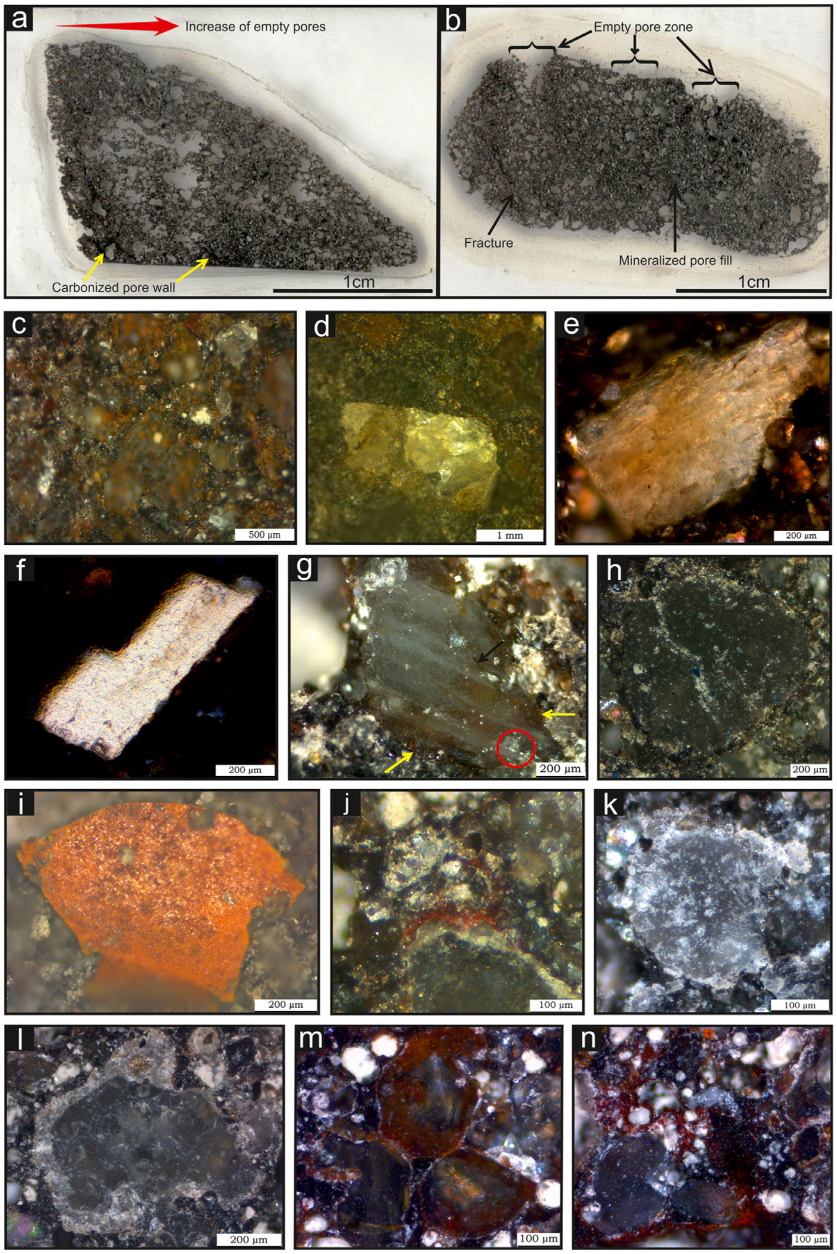

Fig. 6. Reflected and polarized light photomicrographs of the charred bone clast. a: Polished section under reflected light. Sample cut in the longitudinal direction of the charred bone clast exposing the occurrence of completely filled pores along the periphery and gradual increase of empty pores towards the centre; b: Polished section under reflected light. Sample cut across of the charred bone clast exposing the occurrences of bands of empty pores interspersed with relatively stabilized, but carbonized/graphitized bone microstructure walls/bands. Comparison between the longitudinal and cross -sections shows that the pore-fillings of the original bone microstructure progressed from the periphery of the clast during its initial burial and is the reason why the pores in the inner part of the clast are empty. Subsequent exhumation and redeposition in another depositional downstream site, perhaps introduced the clast to relatively dry-hot climate with occasional wetting, that might have contributed toward weathering of the Fe-bearing minerals (see Table 2), the release of iron oxide and coating them on the grain surfaces and pore walls; c: Photomicrograph showing the oxide-coated grains and pore walls; d: Close-up view of the polished section under reflected light showing the pore wall structure, pore-filling and oxide-coated grains within the pores; e: Micropore filled completely with rhombic calcite cement, typical of phreatic zone. Photographed under crossed nicols; f: Close-up view of pore-filling calcite cement showing typical rhombic cleavage; g: Photomicrograph under crossed nicols showing the angular plagioclase grain, probably drawn from proximal source during a major erosional event in the catchment region of the river. Shorter transport distance ensured that the grain got deposited before inheriting roundness. Deposition occurred at the region wherein kankar developed, during which the grain got cemented and later exhumed and redeposited in the downstream region. The grain shows typical cleavage of feldspars, besides fracture (shown by black arrow) that cross-cuts the cleavage planes, oxide coating around the periphery (shown by yellow arrow) and development of weathering product, probably sericite (shown by red circle); h: Photomicrograph showing the pore-fill cross-cut by a late-stage fracture, which in turn was filled with microspars of calcite. These cement spars have undergone destructive neomorphism due to which regionally varying crystal sizes, morphologies and translucent nature were imparted, typifying the neomorphic origin. i: Photomicrograph showing iron oxide patch forming pore-fill within the microstructure of the charred bone clast; j: Photomicrograph showing iron oxide-coating on the pore wall; k: Photomicrograph showing the calcite cement spar as pore-fill that has undergone destructive neomorphism. The ghost structures reveal the compromise structure, i.e., original cement spar character of the calcite spar, that was precipitated in a meteoric phreatic zone that in turn was later subjected to exhumation, transport, redeposition and experienced hot-dry, meteoric vadose zone of alteration/late-stage diagenesis; l: Photomicrograph under crossed nicols showing the pore-filling calcite cement spar that has undergone destructive neomorphism. Pore-filling nature and compromise structure are recognizable as ghost structures. Also, note the destructive neomorphism that approaches from the periphery of the pore-wall towards the centre. Sharp contact between the pore-wall (made up of charred carbon of the bone marrow) and the calcite cement is typically recognizable. Similarly, the reaction frond between the destructive neomorphism and original pore-filling calcite is also discernible through tonal differences and spar morphologies; m: Microphotograph showing oxide-coated grains in a close-up view; n: Microphotograph showing the spread of the oxide coating from the periphery toward the centre and complete occupation. (For interpretation of the references to color in this figure legend, the reader is referred to the web version of this article.)

Table 1
Mineral species recognized in the sediment samples from both the pits of the Vaigai River Basin through the X-Ray Diffraction. Plagioclase: Albite, Oligoclase/both**; **X*** - both orthoclase and microcline; **X+** - Actinolite; **X++**-Hornblende; **Clinopyroxene:** Diopside, Aegirine.

Mineral/Sample No.	AP1-1	AP1-7	AP1-8	KLMB-1	KLMB-2	KLMB-3	KLMB-4	KLMB-5
Quartz/Quartz low		X	X	X	X	X	X	X
Plagioclase		X	X	X	X	X**	X	X
K-Feldspar		X	X*	X	X	X	X	X
Orthopyroxene					X			X
Clinopyroxene		X	X	X		X	X	
Amphibole		X+	X++	X++			X+	X++
Muscovite		X	X	X		X	X	X
Calcite	X							
Apatite	X				X			
Chloroapatite	X							
Illite					X	X		
Montmorillonite							X	
Graphite		X			X		X	
Lanthanite						X		
Zirkelite						X	X	
Sapphirine							X	

Table 2
Radiocarbon ages of selected sediment, charcoal and bone and charred bone clast samples. Ages are presented in calibrated before present (cal yr BP) and Common Era (BCE/CE) scales.

Location/Pit	Sample type	Depth (cm) below surface	Calibrated Radiocarbon Age (cal yr BP)	Calibrated age in Common Era scale at 95.4% Probability (BCE/CE)		
				From	To	Median
Agaram	Bone	170	619 ± 39	1278 CE	1390 CE	1312 CE
Varusanadu#	Organic Carbon	45	729 ± 31	1167 CE	1269 CE	1225 CE
Agaram	Charcoal	198	1321 ± 17	599 CE	659 CE	629 CE
Agaram	Charcoal	216	1353 ± 25	555 CE	644 CE	596 CE
Keezhadi*	Sediment	230	2314 ± 29	412 BCE	237 BCE	390 BCE
Keezhadi*	Sediment	250	2435 ± 34	752 BCE	406 BCE	530 BCE
Keezhadi	Sediment	160	3038 ± 57@	1211 BCE	997 BCE	1082 BCE
Keezhadi	Sediment	240	3543 ± 54@	1613 BCE	1414 BCE	1489 BCE
Keezhadi	Sediment	205	3503 ± 52@	2136 BCE	1620 BCE	1860 BCE
Keezhadi	Sediment	270	4908 ± 192@	3346 BCE	2589 BCE	2961 BCE
Agaram	Sediment	430	4938 ± 84	3307 BCE	2878 BCE	2976 BCE
Keezhadi	Sediment	325	7091 ± 109@	5359 BCE	4942 BCE	5147 BCE
Agaram	Charred Bone clast	200	7455 ± 73	5627 BCE	5370 BCE	5511 BCE

* Data from Ramkumar et al. (2021).
# Data from Ramkumar et al. (2019).
All other data are generated during the present study.
@ Modeled data.

5. Discussion

5.1. Nature and controls of the depositional environments

Plots based on the discriminant lines of Friedman (1967) and Moiola and Weiser (1968) unequivocally suggested riverine origin for the sediments (Figs. 5a and 5b). This inference is substantiated in the discriminant diagram of Stewart (1958), wherein the energy conditions are differentiated based on the relative intensity of energy conditions and direction of flow (unidirectional: river process and bidirectional: wave process). The studied samples plotting within the river process and slow deposition fields reiterated the previous inference of riverine origin. In addition, the discriminant diagram of Stewart (1958) also provided clues to the prevalent variations in energy conditions as a result of changes in flow regime and / or various microenvironments located within a delta system (Fig. 5c; Ramkumar, 2001; Ramkumar and Murty, 2000; Ramkumar et al., 2000). General immature nature of the sediments and their deposition in various microenvironments/geomorphic units of the delta system are affirmed by the samples in the braided bar, point bar, and delta front fields of the discriminant diagram of Glaister and Nelson (1974) (Fig. 5d). These observations also support the inference of changes in depositional regions/microenvironments as well as flow conditions and/or energy conditions. The discriminant plot of transport mode proposed by Passega (1957) suggests variable intensities of the transport (Fig. 5e), perhaps due to the prevalent monsoon-flow controlled nature of the sediment transport. All the samples plot on eastern side of the C = M discriminant line paralleling the field of suspension with rolling mode. Together, they indicate deposition in a deltaic system, probably under the influence of seasonally varying flow conditions, in regions principally juxtaposed in and around a major river channel. The differences between the sample clusters of the Agaram and Keezhadi pits are suggestive of spatial variation of sediment character influenced by variations in sediment transport, deposition, energy and environmental setting.

The lithofacies on a stratigraphic context establish the prevalence of centennial-to-millennial scale channel avulsion producing the alternating/cyclic channel-flood plain deposits intervened by overbank and/or natural levee deposits. These overbank and natural levee surfaces were colonized by humans. The occurrences of bone clasts including charred bone clasts and pot shreds indicate that the deposited sediments did not have a distal provenance, if not exactly from the vicinity. This is inferred based on the fragility of the charred bone clast and its delicate nature to acquire roundness even during short distance transport. Documentation of monotonous granulometric/textural characteristics suggested tectonic quiescence and monsoon driven climatic extreme events over the late Holocene that enforced channel avulsion and resultant marooning and or catastrophic burial of human habitation sites. The subtle changes were indicated by the absolute values, linear and polynomial trends of the sediment characteristics that indicate a drastic shift of environmental conditions, probably corresponding with the major events of flood and habitation abandonment surface followed by gradual restoration of fluvial dynamics and rehabilitation. Evidence of habitation on the overbank and/or natural levee adjoining/juxtaposed the river channel shown in the Agaram and Keezhadi pits suggests a choice of ancient human society for selecting habitation sites. Most of them were marooned and/or destroyed by burial under flood deposits following their abandonment by humans (Figs. 2 and 3). The extreme climatic event(s), exhumations of upstream settlements and depositions of the debris over downstream habitation sites, were possibly episodic and the ancient human society was ignorant and/or ill-prepared about them. In an earlier report, Ramkumar et al. (2021) documented extensive use of the Quaternary-to-Recent kankar and paleosol deposits as preferred burial grounds of the ancient society. They were episodically eroded by the shifting channels, especially during major catastrophic floods and exhumation, transportation and redistribution of the burial urn pot shreds and all other paraphernalia contained in them, including the human bone remains in the resultant younger flood deposits.

The easterly flowing peninsular rivers of southern India are known for catastrophic flooding (Ramkumar et al., 2015b, 2016, 2018). Recently, the religious-cultural site buried under the flood deposit of the Cauvery River and similar site(s) in the apex of the Vaigai River delta were unearthed (Ramkumar et al., 2018, 2021) and affirmed that the Vaigai River, similar to the Cauvery River and Thamirabarani River have marooned historic-prehistoric sites of habitations and buried them under thick flood deposits. The sedimentological inference of highly varied flow conditions and prevalence of extreme flood events associated with climate change played havoc on ancient settlements of the Vaigai Civilization. The clast morphology, microstructure, pore-fillings and inferred paragenetic sequence suggest that the charred bone clast might originally be a human bone, charred by burning, perhaps as a burial ritual representing the mid-Holocene (5511 BCE; 7455 $\pm$ 73 cal yr BP). This oldest human evidence of the Vaigai Civilization in the sedimentary archive of this study was however reworked during the extreme flood events between ca. 629-596 CE (1321-1353 cal yr BP), representing the late Holocene. Documentation of comparable ^{14}C age of carbon-rich sediment layer in the Keezhadi pit supports the inference that the charred bone clast might have been exhumed from the proximal regions of the erstwhile habitation site. The circulated groundwater into the periphery of the charred bone and commencement of precipitation of cement spars in the available pores, occurred under meteoric phreatic conditions, i.e., below the water table. It might have been exhumed by prevalent erosion associated with the flood events and deposited at the sampling site. The compaction-fracturing-cementation in fractures, oxidation, and precipitation of oxide coating along pore walls reflects neomorphism and weathering. Compilation of these events in a genetic-paragenetic sequence suggest plausible initial period of habitation-ritual burial understable climatic conditions and the subsequent unstable conditions caused oxidation of ferromagnesian minerals and enforced weathering and neomorphism due to modified hostrock-circulating fluid conditions.

5.2. Chronology of prehistoric-historic natural and anthropogenic events

The Vaigai River flows on an antecedent valley. The Holocene-Recent sediments of this river rest over paleovalleyfill and kankar. The sprawl of kankar on the surface corresponds to adjoining terraced uplands and /or historic-modern river channel (Ramkumar et al., 2016, 2019). The Quaternary age kankar deposits were incised during the Early Holocene, forming the terraced upland adjoining the river courses (Ramkumar et al., 2019). This information, together with the observation that the kankar deposits served as burial grounds for the Microlithic-Neolithic human societies (Fig. 7; e.g., Ramkumar et al., 2021) suggest habitation and/or utilization of the kankar surface for burial by the ancient human community at least since the early Holocene or Microlithic age. Thus, the burial grounds could be considered as the initial colonization surface/time as they contain three different types of burial/ritual materials. The absolute timeline could be derived from the oldest radiocarbon date of the present study, i.e., the age of charred bone clast recovered from the Agaram pit (5511 BCE; 7455 $\pm$ 73 cal yr BP). Depositions representing river channel, natural levee and overbank sediments with possible avulsion in the Keezhadi pit (5147 BCE; 7091 $\pm$ 109 cal yr BP), and contemporary to the charred bone clast age reflect a relatively stable hydroclimate. This habitation surface in the kankar after nomadic microlithic age hereinafter referred as habitation surface 1 or HS-1. The shifting of the channel courses through avulsions possibly occurred under stable conditions as a result of reduced channel slopes due to less frequent or minimal flooding events and resultant erosions (Ramkumar et al., 2019, 2021). The petrography and microstructure analyses suggest that the charred bone clast got its pores cemented and filled with matrix grains, to be later exhumed, transported and redeposited by flood events between 596-629 CE (1353-1321 cal yr BP).

The next habitation surface/time, referred as HS-2, is related to the carbon rich sediment layer at the Agaram Pit (2976 BCE; 4938 $\pm$ 84 cal yr BP) as well as the contemporary sediment layer at Keezhadi Pit (2961 BCE; 4908 $\pm$ 192 cal yr BP). This habitation surface was buried under the flood deposits and yielded an amalgamation of transported artefacts. The third habitation surface rests over the flood deposit and dated to be around 1860-1489 BCE (3543-3503 cal yr BP). Ramkumar et al. (2021) recorded the fourth habitation surface (HS-4) with an age of 530-390 BCE (2435-2314 cal yr BP). The fifth habitation-colonization (HS-5) was during 596-629 CE (1353-1321 cal yr BP) and the most recent habitation-colonization occurred during post 1225-1312 CE (729-619 cal yr BP). Occurrences of flood deposits superimposing habitation surfaces, for example, HS-1 (5511-5147 BCE), HS-2 (2976 BCE in Agaram and or 2961 BCE in Keezhadi), HS-3 (1860-1489 BCE), HS-4 (530-390BCE), after HS-5, (596-629 CE), and post 729-619 CE suggest episodic flooding and/or marooning as a result of channel avulsion as the cause(s) of erosion-deposition in the Vaigai River system. Attendant was the destruction of the habitation surfaces and the settlements that forced the inhabitants/survivors to move and colonize newer settlements, which were subsequently buried under successive younger flood deposits. Documentation of oxide formation, indicating changing conditions from wet-humid to dry-hot climate suggested that it is imperative to examine the role of climate including extreme climatic events on the survival and abandonment of ancient civilization sites. These inferences are summarized in the Fig. 8.

5.3. Episodic extreme climatic events and destructions of habitation sites

Floodplains and natural levees located along the perennial rivers were the preferred landforms for ancient human settlements (Singh et al., 2017). With the advancements of ancient civilization and population, these settlements grew into well-organized and structured cities. This might be the reason for the unearthing of remnants of the ancient civilizations in river deltaic regimes. In India, the Indus and the Saraswati settlements

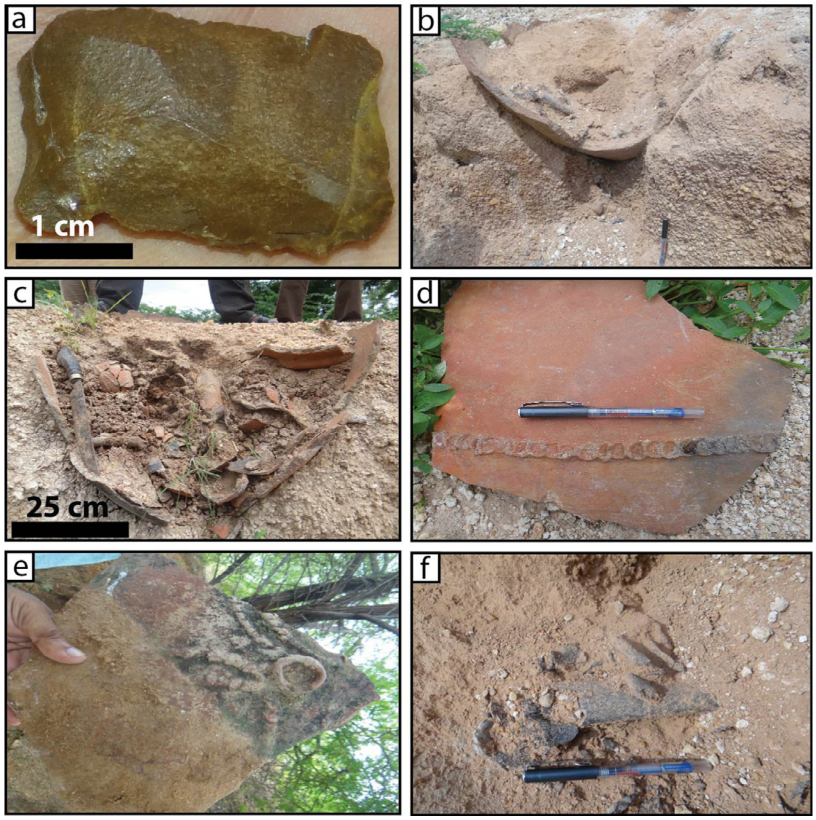

Fig. 7. Field and megascopic evidences of multiple prevalent cultural traits. a: Microlithic stone tool, perhaps used as a small handy blade found at Maranadu. This finding, together with the carbon isotope dates and existence of the modern city of Madurai, suggest continuous habitation in the Vaigai River plains since at least microlithic age until today. b and c: Burial urns found to occur in the kankar. The morphologies, external designs and contents of these are different and are inferred to have been meant for varied customs/communities/social hierarchical groups. d. and e: Burial urns with aesthetic epirelief features. The urns are multifold thicker than all other pot shreds and contain three different types of human bone remains viz., i. charred/burned bone remains without any skull and or complete skeletal remains, ii. bone remains with other utensils/artefacts, perhaps used by the person who might have used and iii. complete bone remains including skull, jaw apparatus, etc. Ramkumar et al. (2021) have documented these and interpreted that these three types of burial characters indicate at least three different cultural traits and or cultural groups that inhabited the region, almost simultaneously, as these are found at similar stratigraphic levels. f. Completely burned/charred bone remains found within a burial urn.

were found along the banks of the Indus River (Giosan et al., 2012, 2018) and the ancient Saraswati River (Radhakrishna and Merh, 1999; Tripathi et al., 2004; Valdiya, 2013). As the settlements located along the water bodies are under the vagaries of seasonal-short and or long-term climatic changes and natural hazards (Singh et al., 2017) the very landforms that support human activities and sustenance, wreak havoc and force the settled communities to shift or vanish from the habitat. These geohazards bury and/or maroon the settlements causing loss of life and infrastructure (e.g., Menier et al., 2017). Extreme weather events exert control over erosion-transportation-deposition processes, and impact landscape development (Bookhagen et al., 2005). The influences of climatic shifts on stream flow have the potential to increase/decrease sediment flux and thus, affect riverbed elevation by altering flood frequency (Slater and Singer, 2013) and magnitude (Ramkumar, 2009). The sudden/faster and unforeseen bed elevation events (Slater and Singer, 2013; Thakur et al., 2016) and subsequent and or associated changes in stream courses and marooning of adjoining regions as responses to climate change and extreme climatic events have important implications for survival-demise/burial of ancient civilization sites located along the riverbanks (Ramkumar et al., 2015a, 2015b, 2018, 2019).

The natural cataclysms such as earthquakes, landslides, volcanic eruptions, tsunamis, droughts and coastal and fluvial flooding have affected the modern as well as ancient human societies. The developments of scientific methods and instrumentation over the past decades have helped to mitigate their effects and reduce the loss of life. The lack of natural hazard preparedness of our ancestors might have made them highly vulnerable causing loss of life and infrastructure, including settlements. The climate variation and coeval development-destruction of civilization sites and exodus-migration of the human race are well documented (e.g., DeMenocal, 2001; Butzer, 2012; Weiss, 2016; Giesche et al., 2019; Mehrotra et al., 2019). In India, the thick fortifications found in the Dolavira city walls were the results of the prevalent awareness among the inhabitants and mitigation effort against geohazards including tsunami (Nigam et al., 2016) and storms (Nigam and Chaturvedi, 2006). Roy and Sethumadhav (2014) and Valdiya (2008) argued that the prevalent neo-morphotectonics in catchment of the Cauvery River were the reasons for the burial of man-made infrastructure. Similarly, Roy et al. (2017) reported destruction and abandonment of villages in Jaisalmer due to paleoseismicity that occurred about 200 years ago. Paleoseismicity has also been attributed to the devastations of ancient civilization sites at Sagalassos, Southwest Turkey (Similox-Tohon et al., 2006). According to Rao (1991), catastrophic floods have devastated the ancient Harappa cities at Dolavira. Singh et al. (2017) documented multiple ancient civilization sites along the paleochannels of the Indus and the Sutlej. They have also opined that the stream avulsions (i.e., shifting of stream courses in the flood plains on a century, millennial and longer time scales) have caused diversion of stream flow along the new and/or paleochannel courses, which could be considered as one of the causes for abandonment of ancient settlements. Examination of paleolithic-historic archae-

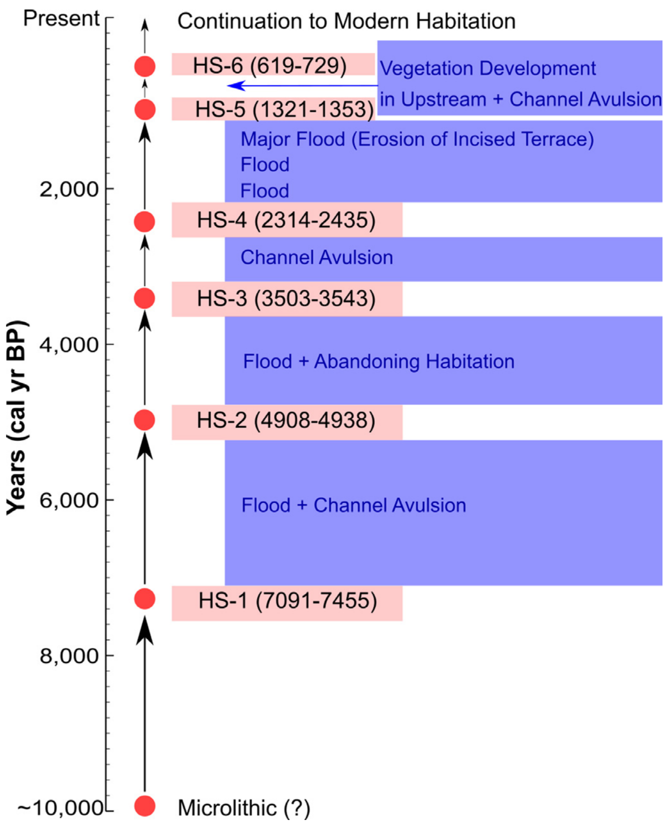

Fig. 8. Chronology of habitations interspersed with channel avulsion and flooding events. In addition to the episodic habitations and abandonments interspersed with flooding and channel avulsion continuum of habitation of the Vaigai River flood plains could also discerned from this figure.

ological sites in Tamil Nadu state of southern India suggests extensive occurrences of archaeological sites in the deltahead region, and their ubiquitous occurrences below catastrophic flood deposits (e.g., Ramkumar et al., 2018, 2019) necessitate the role of exogenic forcing including that of extreme climate events. The catastrophic floods in the Upper Cauvery River were either controlled by periods of intense climate change and/or superimposed on paleo-present seismically active zones (Kale et al., 2010; Ramkumar et al., 2016). Few of the flood events that wrecked havoc and destroyed ancient habitats found their mention in cave carvings/paintings, stone inscriptions, inscriptions on palm leaves, and copper plates, and Sangam literature representing 11000-2000 years BP.

Flood chronologies developed across the world have shown that even minor changes in the climatic patterns can be associated with more frequent occurrences of extreme flood events (Kale et al., 2010; Knox, 2000). Independent studies of Kale et al. (2010), Ramkumar et al., (2018), and Goswami et al., (2019) documented the flood deposits of the Cauvery River and found distinct flood clusters occurred during the times of major shifts in the monsoon conditions, from fluvial dormancy to sudden outburst of monsoons (~2 ka), from warmer to colder (onset of ‘Little Ice Age’ (LIA) ~ 14th century), from colder to warmer (end of LIA ~ 19th century) and ~20th century, indicating that the climatic pattern can be associated with more frequent occurrences of extreme flood events. The study of Kale et al. (2010) also showed that the two major flood events of the 20th century reported from the upper Cauvery were produced by high-intensity short-duration storms, suggesting that not all wet phases are associated with major floods and all dry phases with low floods/droughts.

In this context and precedents, documentation of flood deposits in the studied sites located in the Vaigai River Basin, from upper to downstream regions and associated shifts in river channel affirm the dominance of climatic reversals and or extreme climatic events on the development and destruction of ancient settlements of the Vaigai Civilization, as could be found elsewhere including India (e.g., Giosan et al., 2012, 2018; Giesche et al., 2019). Previous studies have established the relationship between enhanced erosion and the influx of excessive sediments into the trunk channel due to the landuse changes (Ramkumar et al., 2015a, 2015c). These excessive sediments can be flushed out of the channel during extreme flooding (Ramkumar, 2000, 2003). They also become the cause of bank breach and channel avulsion (Ramkumar et al., 2015b). Giosan et al. (2012) showed that the monsoon-fed rivers were active during the Holocene. As the monsoon weakened, monsoonal rivers gradually dried or became seasonal, affecting habitability of the ancient societies that were located along the river courses. Present observations in terms of episodic stream avulsion, marooning of ancient habitation sites/surfaces under flood deposits, and subsequent abandonment of habitation sites also evince a strong relationship between tectono-climatic factors on the river systems and thus, on the survival-abandonment of ancient habitation sites, especially in the plains of the Vaigai River.

On a geological, pre-historic and historic scale, the Vaigai River was a dryland river, the dynamics of which might be different from that of rivers flowing in the humid regions. According to Tooth (2000), the dryland rivers have unique fluvial environments, hillslope and channel hydrological and sediment transport processes, river pattern and geometry, temporal and spatial aspects of channel change, sedimentary structures and bedforms that contrast with more humid fluvial environments. The dryland rivers experience extreme temporal and spatial variability of rainfall, runoff and sediment transport, and poor integration between tributary and trunk channels and the same has been reported for the Vaigai River on a centennial scale (Ramkumar et al., 2018). Above all, large floods control the channel morphology of the dryland rivers. This uniqueness might have played a significant role in channel avulsion in the downstream reaches of the Vaigai River and played havoc on ancient settlements since pre-historic times. The occurrences of flood events at about 200-300 year intervals as indicated by flood deposits immediately almost every habitation surface, for example, after HS-1 (5511-5147 BCE), after HS-2 (2976 BCE in Agaram and 2961 BCE in Keezhadi), after HS-3 (1860-1489 BCE), HS-4 i.e., post 530-390 BCE, after HS-5, i.e., between 596-629 CE, and 1225-1312 CE concur with the findings of Zhao et al. (2015) who have documented variations in low-latitude monsoon precipitation driven by shifts in the mean position of the intertropical convergence zone (ITCZ), which is further mediated by solar activity and tropical sea surface temperature . These authors have also stated that the Asian Southern Monsoon has 220-year cyclicity concordant with the dominant cycle of solar activity (Zhao et al., 2015). However, in order to ascertain this presumption, very-high resolution age control is required.

The ancient city of Madurai in southern India has been under habitation for many tens of centuries. This city found its mention in the writings of Magasthenes (who visited the city during 300 BCE), Pliny the Younger (61-112 BCE), and Ptolemy (90-168 BCE) and Indian chroniclers such as Kautila’s Arthashastra (370-283 BCE), and Sangam Literature (1200-100 BCE). Since then, various parts of the Madurai continue to be inhabited along the Vaigai River until Recent and our study attests to the continuous habitation since the microlithic age (Fig. 6 and Fig. 7). The Sangam literature also mentions the havoc caused on agricultural fields and ancient settlements by periodic flooding (Ramkumar et al., 2018,

2021) of the Vaigai River and resultant mitigation efforts and shifting of settlements of kings of yore.

6. Conclusions

The Vaigai River Basin in southern India is one of the continually habilitated regions, and the sedimentary deposits have provided evidence of microlithic-historic-recent settlements, hunting-modern industries, agricultural and other structures. The previously published evidence of habitation in the Vaigai River Basin during the microlithic age, combined with the present report of six habitation surfaces/sites/events namely, 5511-5147 BCE (7455-7091 cal yr BP), 2976-2961 BCE (4938-4908 cal yr BP), 1860-1489 BCE (3543-3503 cal yr BP), 530-390 BCE (2435-2314 cal yr BP), 596-629 CE (1353-1321 cal yr BP) and post 1225-1312 CE (729-619 cal yr BP) suggest habitation and abandonment of the flood plains of the Vaigai River over the mid to late Holocene were episodic and were subjected climate-related flooding and stream avulsion. Implications of these results together with our previous studies could be that while the evidences of urbanism, industrial and leisure activities documented are comparable with other contemporaneous known civilizations elsewhere, evidences of cohabitation of multiple societal groups that practiced varied burial customs make the Vaigai Civilization an unique one. In addition, the practice of ritualistic burning-burial of deceased are also documented by the present study and the carbon isotopic age for the charred bone suggested the prevalence of this practice in the Vaigai Civilization much earlier than other Civilizations of the World. These conclusions necessitate integrated, systematic, very-high resolution climatic, geomorphic, habitation and archaeo-cultural studies.

Credit author statement

MR planned, executed the research, interpreted the data, drafted and finalized the manuscript. MR, KB and KK planned and coordinated the field work and subsequent laboratory analyses. MS, PDR and RN participated in the interpretation of data and manuscript drafting. AM and SL took part in sample collection, AM, CR and KJJ conducted granulometric analyses and sample preparation for other analyses. NAS took part in log preparation and drafting manuscript. RS, PK and SC analyzed the samples for geochronology and mineralogy and participated in drafting and checking the manuscript text. All the authors corresponded, contributed and modified the text of the manuscript.

Acknowledgements

The authorities of Periyar University and the Department of Archaeology, State Government of Tamil Nadu are thanked for according necessary administrative permission to conduct field investigations and sampling campaigns. Few of the photographs of artefacts are recovered by the archaeological department personnel who accompanied senior authors during the field survey. The MoU's signed between the Periyar University and the University of South Brittany, France, Curtin University Sarawak, Malaysia and Universiti Teknologi Petronas facilitated collaborative work and the authors are thankful for the same. Authors are thankful to IUAC for extending AMS facility for ^{14}C funded by Ministry of Earth Science (MoES), Government of India (reference numbers MoES/16/07/11(i)-RDEAS and MoES/P.O.(Seismic)8(09)-Geochron/2012). The authors are thankful to Malvern Panalytical for providing two High-Score software licenses for a year. We thank the editor and two anonymous reviewers for constructive criticisms and suggestions.

References

Bathurst, R.G.C., 1972. Carbonate sediments and their diagenesis. In: Developments in Sedimentology, 12. Elsevier, pp. 1–658.
Bathurst, R.G.C., 1987. Diagenetically enhanced bedding in argillaceous platform limestones: stratified cementation and selective compaction. Sedimentology 34, 749–778.
Bookhagen, B., Thiede, R.C., Strecker, M.R., 2005. Abnormal monsoon years and their control on erosion and sediment flux in the high, arid northwest Himalaya. Earth Planet. Sci. Lett. 231, 131–146.
Bronk Ramsey, C, 2009. Bayesian analysis of radiocarbon dates. Radiocarbon 51 (1), 337–360. doi:10.1017/S0033822200033865.
Butzer, K.W., 2012. Collapse, environment, and society. In: Proceedings of the National Academy of Sciences, 109, New York, pp. 3632–3639.
Chase, B., Meiggs, D., Ajithprasad, P., 2020. Pastoralism, climate change, and the transformation of the Indus Civilization in Gujarat: faunal analyses and biogenic isotopes. J. Anthropol. Archaeol. 59, 1011173 https://doi.org/10.1016/j.jaa.2020.101173.
DeMenocal, P.B., 2001. Cultural responses to climate change during the late Holocene. Science 292, 667–673.
Friedman, G.M., 1967. Dynamic processes and statistical parameters compared for size frequency distribution of beach and river sands. J. Sediment. Petrol. 37, 327–354.
Gao, P., Santosh, M., Yang, C-X., Kwon, S., Ramkumar, M., 2021. High Ba–Sr adakitic charnockite suite from the Nagercoil Block, southern India: Vestiges of Paleoproterozoic arc and implications for Columbia to Gondwana. Geosci. Front. 12, 101126. doi:10.1016/j.gsf.2020, 12.007.
Giesche, A., Staubwasser, M., Petrie, C.A., Hodell, D.A., 2019. Indian winter and summer monsoon strength over the 4.2 ka BP event in foraminifer isotope records from the Indus River delta in the Arabian Sea. Clim. Past 15, 73–90.
Giosan, L., Clift, P.D., Macklin, M.G., Fuller, D.Q., Constantinescu, S., Durcan, J.A., Stevens, T., Duller, G.A.T., Tabrez, A.R., Gangal, K., Adhikari, R., Alizai, A., Filip, F., Van Laningham, S., Syvitski, J.P.M., 2012. Fluvial landscapes of the Harappan civilization. Proc. Natl. Acad. Sci. 109, E1688–E1694.
Giosan, L., Orsi, W.D., Coolen, M., Wuchter, C., Dunlea, A.G., Thirumalai, K., Munoz, S.E., Clift, P.D., Donnelly, J.P., Galy, V., Fuller, D.Q., 2018. Neoglacial climate anomalies and the Harappan metamorphosis. Clim. Past Discuss 1–30. doi:10.5194/cp-2018-37.
Glaister, R.P., Nelson, H.W., 1974. Grain size distribution: an aid in facies classification. Bull. Can. Petrol. Geol. 22, 203–240.
Goswami, K., Rawat, M., Jaiswal, M.K., Kale, V.S., 2019. Luminescence chronology of late-Holocene palaeofloods in the upper Kaveri Basin, India: An insight into the climate-flood relationship. Holocene 29, 1094–1104. doi:10.1177/0959683619831436.
GSI, 1975. Geology of parts of Madurai, Nilakkottai and Tirumangalam Taluks. Geological Survey of India, Madurai District, Tamil Nadu. SROGSI 5428 http://nwm.gov.in/sites/default/files/Vaigai_Basin-17.07.17.pdf.
Haug, G.H., Guenther, D., Peterson, L.C., Sigman, D.M., Hughen, K.A., Aeschlimann, B., 2003. Climate and the collapse of Maya Civilization. Science 299, 1731–1735.
Kale, V.S., Achyuthan, H, Jaiswal, M.K., Sengupta, S., 2010. Palaeoflood records from upper Kaveri River, southern India: evidence for discrete floods during Holocene. Geochronometria 37, 49–55.
Knox, J.C., 2000. Sensitivity of modern and Holocene floods to climate change. Quat. Sci. Rev. 19, 439–457.
Longin, R., 1971. New Method of Collagen Extraction for radiocarbon Dating. Nature 231, 241–242.
Malik, N., 2020. Uncovering transitions in paleoclimate time series and the climate driven demise of an ancient civilization. Chaos 30, 083108. doi:10.1063/5.0012059.
Mehrotra, N., Shah, S.K., Basavaiah, N., Laskar, A.H., Yadava, M.G., 2019. Resonance of the '4.2ka event' and terminations of global civilizations during the Holocene, in the palaeoclimate records around PT Tso Lake, Eastern Himalaya. Quat. Int. 507, 206–216.
Medina-Elizalde, M., Burns, S.J., Lea, D.W., Asmerom, Y., von Gunten, L., Polyak, V., Vuille, M., Karmalkar, A., 2010. High resolution stalagmite climate record from the Yucatán Peninsula spanning the Maya terminal Classic Period. Earth Planet. Sci. Lett. 298, 255–262.
Menier, D., Manoj, M.J., Pubellier, M., Sapin, F., Delcaillau, B., Siddiqui, N., Ramkumar, M., Santosh, M., 2017. Landscape response to progressive tectonic and climatic forcing in NW Borneo: Implications for geological and geomorphic controls on flood hazard. Nat. Geosci. Rep. 7, 457. http://doi.org/10.1038/s41598-017-00620-y.
Moiola, R.J., Weiser, D., 1968. Textural parameters: an evaluation. J. Sediment. Petrol. 38, 45–53.
Nigam, R., Chaturvedi, S.K., 2006. Do inverted depositional sequences and allochthonous foraminifers in sediments along the coast of Kachchh, NW India, indicate palaeostorm and/or tsunami effects? Geo. Mar. Lett. 26, 40–52.
Nigam, R., Dubey, R., Saraswat, R., Sundaresh, A., Gaur, A.S., Loveson, V.J., 2016. Ancient Indians (Harappan settlement) were aware of tsunami/storm protection measures: a new interpretation of thick walls at Dholavira, Gujarat, India. Curr. Sci. 111, 2040–2043.
Passega, R., 1957. In: Texture as Characteristic of Clastic Deposition, 41. American Association of Petroleum Geologists Bulletin, pp. 1952–1984.
Radhakrishna, B.P. and Merh, S.S., (Eds.) 1999 Vedic Saraswati- Evolutionary History of a Lost River of Northwestern India. Memoirs of the Geological Society of India 42, 329.

Ramkumar, M., 2000. Recent changes in the Kakinada spit, Godavari delta. J. Geol. Soc. India 55, 183–188.
Ramkumar, M., 2001. Sedimentary environments of the modern Godavari delta: characterization and statistical discrimination towards computer assisted environment recognition scheme. J. Geol. Soc. India 57, 49–63.
Ramkumar, M., 2003. Progradation of the Godavari delta: a fact or empirical artifice? Insights from coastal landforms. J. Geol. Soc. India 62, 290–304.
Ramkumar, M., 2007. Spatio-temporal variations of sediment texture and their influence on organic carbon distribution in the Krishna estuary, India. Indian J. Geochem. 22, 143–154.
Ramkumar, M., 2008. Carbonate diagenesis in the Kallankurichchi Formation, Ariyalur Group, South India and its implications on petroleum prospects. J. Geol. Soc. India 71, 407–418.
Ramkumar, M., 2009. Flooding - A manageable geohazard. In: Ramkumar, M. (Ed.), (Editor) Geological Hazards: Causes, Consequences And Methods of Containment. New India Publishers, pp. 177–190.
Ramkumar, M., Murty, M.V., 2000. Distinction of sedimentary environments of the Godavari delta using geochemical and granulometric data through analysis of variance (ANOVA). Indian J. Geochem. 15, 69–84.
Ramkumar, M., Sudharani, P, Gandhi, M.S., Pattabhiramayya, M., Rajanikumari, V., Bhagavan, K.V.S., Swamy, A.S.R., 2000. Textural characteristics of coastal sedimentary environments of the modern Godavari delta. J. Geol. Soc. India 56, 471–487.
Ramkumar, M., Alberti, M., Fürsich, F.T., Pandey, D.K., 2013. Depositional and diagenetic environments of the Dhosa Oolite Member (Oxfordian), Kachchh Basin, India, based on Petrographic data: Implications on the origin and occurrence of ooids and their correlation with global oolite peak. In: Ramkumar, M. (Ed.), On a Sustainable Future of the Earth's Natural Resources. Springer-Verlag., Heidelberg, pp. 179–230 DOI10.1007/978-3-642-32917-3_11.
Ramkumar, M., Kumaraswamy, K., Mohanraj, R., 2015a. Environmental Management of River Basin Ecosystems. Springer-Verlag, p. 761.
Ramkumar, M., Kumaraswamy, K., Arthur James, R., Suresh, M., Sugantha, T., Jayaraj, L., Mathiyalagan, Saraswathi, M., Shyamala, J., 2015b. Sand mining, channel bar dynamics and sediment textural properties of the Kaveri River, South India: Implications on flooding hazard and sustainability of the natural fluvial system. In: Ramkumar, M., Kumaraswamy, K., Mohanraj, R. (Eds.), (Editors) Environmental management of river basin ecosystems. Springer-Verlag, pp. 283–318.
Ramkumar, M., Kumaraswamy, K., Mohanraj, R., 2015c. Land use dynamics and environmental management of River Basins with emphasis on deltaic ecosystems: Need for integrated study based development and nourishment programs and institutionalizing the management strategies. In: Ramkumar, M., Kumaraswamy, K., Mohanraj, R. (Eds.), (Editors). Environmental management of River Basin ecosystems. Springer-Verlag, Heidelberg, pp. 1–20. doi:10.1007/978-3-319-13425-3-1.
Ramkumar, M., Menier, D., Mathew, M.J., Santosh, M., 2016. Geological, geophysical and inherited tectonic imprints on the climate and contrasting coastal geomorphology of the Indian peninsula. Gondwana Res. 36, 52–80.
Ramkumar, M., Kumaraswamy, K., Balasubramani, K., Abdul Rahaman, S., Jegankumar, R., Kumara Ganesh, U., Manikandan, E., Balasundareshwaran, A., Prithiviraj, G., Ayyanthurai, R., Santosh, M., Nagarajan, R., Siddiqui, N.A., Menier, D., Mathew, M.J., Ramachandran, C., Sathyaseelan, M., Sivakumar, P., 2018. Discovery of buried historical structures through integrated geological and geophysical techniques in the Kaveri-Kollidam interfluve, India: Implications for morpho–tectonics and archeological exploration. Archaeol. Prospect. 26, 58–73.
Ramkumar, M., Santosh, M., Abdul Rahaman, S., Balasundareshwaran, A., Balasubramani, K., Mathew, M.J., Sautter, B., Siddiqui, S.N., Usha, K., Sreerhishiya, K., Prithiviraj, G., Nagarajan, R., Thirukumaran, V., Menier, D., Kumaraswamy, K., 2019. Tectono-morphological evolution of the Cauvery, Vaigai and Thamirabarani river basins: Implications on timing, stratigraphic markers, relative roles of intrinsic and extrinsic factors and transience of Southern Indian landscape. Geol. J. 54, 2870–2911. doi:10.1002/gj.3520.
Ramkumar, M., Kumaraswamy, K., Balasubramani, K., Nagarajan, R., Santosh, M., Abdul Rahman, S., Arun Prasad, K., Juni, K.J., Al Fathima, Siddiqui, N.A., Mathew, M.J., Menier, D., Sautter, B., Sharma, Rajveer, Kumar, Pankaj, Chopra, Sundeep, Jegankumar, R., 2021. Neolithic cultural sites and extreme climate related channel avulsion: evidence from the Vaigai River Basin, Southern India. J. of Archaeol. Sci. Rep., (in press).
Rao, S.R., 1991. Dawn and devolution of the Indus civilization. Aditya Prakashan, p. 392.
Roy, A.B., Sethumadhav, M.S., 2014. The 'mystic' sand dune-covered temples of Talakad, Mysore district, Karnataka: evidence of earthquake-related destruction. Curr. Sci. 107, 246–254.
Roy, A.B., Bhu, H., Sharma, P., Vaishnav, K., 2017. Deserted nineteenth century Paliwal villages around Jaisalmer, western Rajasthan, India: historical evidence of palaeoseismicity. Curr. Sci. 112, 402–405.
Roy, P.D., Torrescano-Valle, N., Islebe, G.A., Gutiérrez-Ayala, L.V., 2017. Late Holocene hydroclimate of the western Yucatan Peninsula (Mexico). J. Quat. Sci. 32, 1112–1120.
Roy, P.D., García-Arriola, O.A., Garza-Tarazon, S., Vargas-Martínez, I.G., Muthusankar, G., Giron-García, P., Sánchez-Zavala, J.L., Macias-Romo, M.C., 2020. Late Holocene depositional environments of Lake Coatetelco in Central-Southern Mexico and comparison with cultural transitions at Xochicalco. Palaeogeogr. Palaeoclimatol. Palaeoecol. 560, 110050 https://doi.org/10.1016/j.palaeo.2020.110050.
Santosh, M., Tsunogae, T., Yang, C.X., Han, Y.S., Hari, K.R., Prasanth, M.M., Uthup, S., 2020. The Bastar craton, central India: a window to Archean–Paleoproterozoic crustal evolution. Gondwana Res. 79, 157–184.
Sharma, R., Umapathy, G.R., Kumar, P., Ojha, S., Gargari, S., Joshi, R., Chopra, S., Kanjilal, D., 2019. AMS and upcoming geochronology facility at Inter University Accelerator Centre (IUAC), New Delhi, India. Nucl. Instrument. Methods B 438, 124–130.
Similox-Tohon, D., Sintubin, M., Muchez, P., Verhaert, G., Vanneste, K., Fernandez, M., Vandycke, S., Vanhaverbeke, H., Waelkens, M., 2006. The identification of an active fault by a multidisciplinary study at the archaeological site of Sagalassos (SW Turkey). Tectonophysics 420, 371–387.
Singh, A., Thomsen, K.J., Sinha, R., Buylaert, J.P., Carter, A., Mark, D.F., Mason, P.J., Densmore, A.L., Murray, A., Jain, M., Paul, D., Gupta, S., 2017. Counter-intuitive influence of Himalayan river morphodynamics on Indus civilization urban settlements. Nat. Commun. 8. http://doi.org/10.1038/s41467-017-01643-9.
Slater, L.J., Singer, M.B., 2013. Imprint of climate and climate change in alluvial riverbeds: Continental United States, 1950-2011. Geology 41, 595–598.
Sofia, G., Nikolopoulos, E.I., 2020. Floods and rivers: a circular causality perspective. Sci. Rep. 10, 5175. doi:10.1038/s41598-020-61533-x.
Stewart Jr., H.B., 1958. In: Sedimentary Reflections on Depositional Environment in San Migne Lagoon, 42. American Association of Petroleum Geologists Bulletin, Baja California, Mexico, pp. 2567–2618.
Stuiver, M., Polach, H.A., 1977. Discussion: reporting of C data. Radiocarbon 19, 355–363.
Thakur, S., Chudasama, B., Porwal, A., González-Álvarez, I., 2016. Sub-surface paleochannel detection in DeGrussa area, Western Australia, using thermal infrared remote sensing. In: Khanbilvardi, R., Ganju, A., Rajawat, A.S., Chen, J.M. (Eds.), (Editors) Land Surface and Cryosphere Remote Sensing III 98772C http://doi.org/10.1117/12.2223626.
Tooth, S., 2000. Process, form and change in dryland rivers: a review of recent research. Earth Sci. Rev. 51, 67–107.
Tripathi, J.K., Bock, B., Rajamani, V., Eisenhauer, A., 2004. Is River Ghaggar, Saraswati? Geochemical constraints. Curr. Sci. 87, 1141–1145.
Valdiya, K.S., 2008. Sinking of ancient Talakad temples on the Kaveri Bank, Mysore Plateau, Karnataka. Curr. Sci. 95, 1675–1676.
Valdiya, K.S., 2013. The River Saraswati was a Himalayan-born river. Curr. Sci. 104, 42–54.
Weiss, H., 2016. Global megadrought, societal collapse and resilience at 4.2-3.9 ka BP across the Mediterranean and West Asia. Pages 24, 62–63.
Zhao, K., Wang, Y., Edwards, R.L., Cheng, H., Liu, D., Kong, X., 2015. A high-resolved record of the Asian summer monsoon from Donggecave, China for the past 1200 years. Quat. Sci. Rev. 122, 250–257.